

Cite this: *RSC Adv.*, 2019, 9, 11851Received 28th February 2019  
Accepted 8th April 2019

DOI: 10.1039/c9ra01532a

rsc.li/rsc-advances

# Facile synthesis of aminated indole-based porous organic polymer for highly selective capture of CO<sub>2</sub> by the coefficient effect of $\pi$ - $\pi$ -stacking and hydrogen bonding†

Qiang He, \* Yi Xu and Xiaoqiang Yang

A new aromatic aminated indole-based porous organic polymer, PIN-NH<sub>2</sub>, has been successfully constructed, and it was demonstrated that the coefficient effect endows this porous material with outstanding CO<sub>2</sub> adsorption capacity (27.7 wt%, 1.0 bar, 273 K) and high CO<sub>2</sub>/N<sub>2</sub> (137 at 273 K and 1 bar) and CO<sub>2</sub>/CH<sub>4</sub> (34 at 273 K and 1 bar) selectivity.

Today, one of the most serious environmental problems is climate change, such as global warming and sea-level rises, which are caused by increased concentrations of carbon dioxide (CO<sub>2</sub>) in the atmosphere.<sup>1-3</sup> As we all know, CO<sub>2</sub> mainly arises from fossil-fuel combustion in power plants, and the flue gas is always mixed with other gases including nitrogen (N<sub>2</sub>), methane (CH<sub>4</sub>) and so on. Therefore, it is necessary to design materials for selectively separating and adsorbing CO<sub>2</sub> from these industrial and energy-related sources to improve the environmental problems.<sup>4-6</sup> Aqueous amine solutions are the most common adsorbents for CO<sub>2</sub> separation and capture,<sup>7</sup> however, not only do these adsorbents degrade over time and are corrosive, toxic, and volatile, but also the regeneration process is highly energy demanding for these systems due to the chemical capture mechanism. As alternatives, porous organic polymers (POPs)<sup>8-10</sup> relying on physical adsorption have become the research focus due to their low density, large specific surface area, good thermal stability, and narrow pore size distribution, but the low uptake capacity, and especially, the poor selectivity are two urgent issues that need to be addressed that seriously restrict the commercialization of POP adsorbents.<sup>11</sup> Hence, in the past few years, many methods have been developed to improve the POP performance including increasing the surface area and adjusting the pore size.<sup>12,13</sup>

Recently, based on the rapid development of supramolecular interactions<sup>14,15</sup> and the unique advantage of POP materials, *i.e.*, the structure designability, researchers found that introducing

special active sites into the framework, such as heteroatoms and diverse organic groups, is a simple and effective way to ameliorate the adsorption performance by the formation of some special non-covalent interactions and various functional groups have been explored.<sup>16-18</sup> Recently, Chang *et al.*<sup>19</sup> have designed and prepared an novel aerogel (PINAA) that contains both amide and indole groups and they demonstrated that the CO<sub>2</sub> can be rapidly adsorbed on the heteroaromatic ring of indole because of its relatively large binding area *via* strong  $\pi$ - $\pi$ -stacking interactions, and then, the desorbed CO<sub>2</sub> molecule can be captured by an adjacent amide group because of “electrostatic in-plane” interaction. This synergistic effect of electrostatic in-plane and dispersive  $\pi$ - $\pi$ -stacking interactions of amide and indole with CO<sub>2</sub> endows the resulting aerogel enhanced CO<sub>2</sub> adsorption capacity and CO<sub>2</sub>/CH<sub>4</sub> and CO<sub>2</sub>/N<sub>2</sub> selectivity. Inspired by this fascinating study, we hypothesized that when the indole group is aminated, the CO<sub>2</sub> can be rapidly adsorbed on the heteroaromatic ring of indole because of its relatively large binding area *via* strong  $\pi$ - $\pi$ -stacking interaction (Fig. 1a), after that, the hydrogen bonding interactions between the O of the CO<sub>2</sub> and -NH of the aniline group would make the CO<sub>2</sub> to further form a stable conformation with the aminated indole system (Fig. 1b), as a result, the coefficient effect of  $\pi$ - $\pi$ -stacking interactions and hydrogen bonding interactions would ensure the high CO<sub>2</sub> adsorption capacity and further enhanced CO<sub>2</sub>/CH<sub>4</sub> and CO<sub>2</sub>/N<sub>2</sub> selectivity.

To verify our suppose, in this work, we tactfully designed and fabricated an aminated indole-based aerogel PIN-NH<sub>2</sub> *via* Friedel-Crafts alkylation (Fig. 1c), and its CO<sub>2</sub> adsorption capacity and CO<sub>2</sub>/CH<sub>4</sub> and CO<sub>2</sub>/N<sub>2</sub> selectivity were immediately investigated. The successful preparation of PIN-NH<sub>2</sub> was confirmed by Fourier transform infrared spectroscopy (FT-IR) and <sup>13</sup>C solid state cross-polarization magic-angle-spinning nuclear magnetic resonance (<sup>13</sup>C CP/MAS NMR) spectrometer, and the results are in good agreement with the proposed structures (Fig. S1 and S2,

School of Aviation Engineering Institute, Civil Aviation Flight University of China, Guanghan, 618307, People's Republic of China. E-mail: heqiangxy@126.com

† Electronic supplementary information (ESI) available: Details of materials, measurements and gas adsorption tests; synthesis and characterizations of PIN-NH<sub>2</sub> aerogel; thermal properties, XRD and gas selectivities at 291 and 303 K and isosteric heat of CO<sub>2</sub> adsorption of PIN-NH<sub>2</sub> aerogel; the dynamic breakthrough separation curves; the details of the simulation calculation. See DOI: 10.1039/c9ra01532a



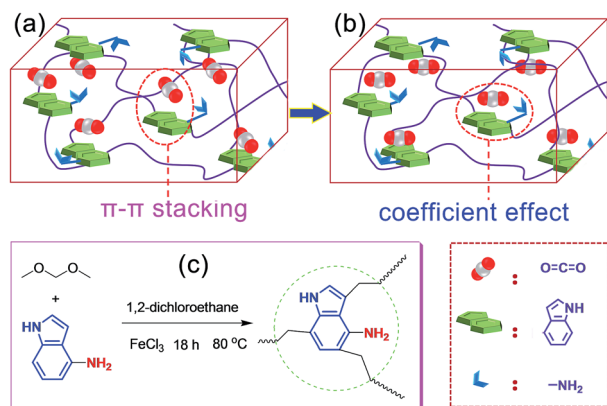


Fig. 1 Schematic representation showing the heteroaromatic ring of indole adsorbing  $\text{CO}_2$  via  $\pi$ - $\pi$ -stacking interactions (a) and the  $\text{CO}_2$  molecule is further stabilized via the coefficient effect of  $\pi$ - $\pi$ -stacking interactions and hydrogen bonding interactions (b). (c) Synthetic route of PIN- $\text{NH}_2$  aerogel.

ESI $\dagger$ ). In the  $^{13}\text{C}$  CP/MAS NMR spectrum of PIN- $\text{NH}_2$ , the peaks at 169–103 ppm are ascribed to the indole group carbons, and the signals located at 35–40 ppm are assigned to the methylene carbons (Fig. S1, ESI $\dagger$ ). For FT-IR spectrum (Fig. S2, ESI $\dagger$ ), the peak at  $3438\text{ cm}^{-1}$  is attributed to the stretching vibrations of N-H in amine unit and indole amine. The peaks at  $2999\text{ cm}^{-1}$  and  $2927\text{ cm}^{-1}$  are assigned to the stretching vibration of  $-\text{CH}_2-$  in the polymer network and the peaks at  $1630\text{ cm}^{-1}$  and  $1480\text{ cm}^{-1}$  are ascribed to the vibrations of the aromatic ring skeleton.

The porosity of PIN- $\text{NH}_2$  was quantified by scanning electron microscopy (SEM), high-resolution transmission electron microscopy (TEM) and  $\text{N}_2$  adsorption-desorption isotherms at 77 K. As shown in Fig. 2a, the SEM image displays that the PIN- $\text{NH}_2$  consists of aggregated particles with sub-micrometer sizes.

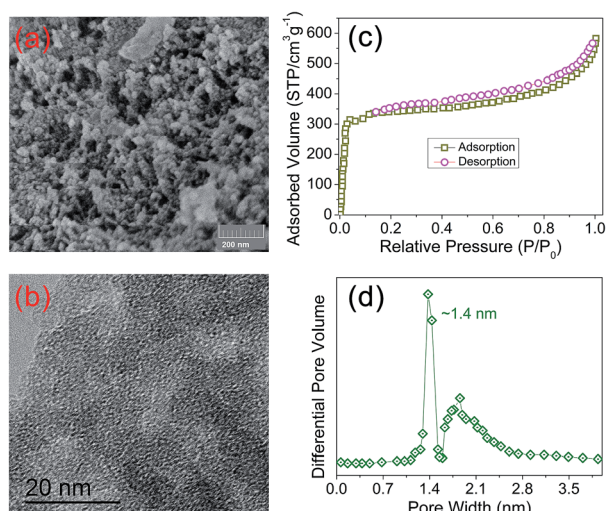


Fig. 2 The microstructures of PIN- $\text{NH}_2$  framework. (a) SEM, (b) TEM, (c) the nitrogen adsorption-desorption isotherms and (d) the pore size distribution of PIN- $\text{NH}_2$  framework.

And the microporous characteristic can be observed clearly from the TEM image as shown in Fig. 2b, the presence of porous structure provides the essential condition for  $\text{CO}_2$  capture and separation. As shown in Fig. 2c, at a low pressure (0–0.1 bar), there is a rapid raise in the  $\text{N}_2$  adsorption-desorption isotherm, indicating its microporous nature, and the increase in the  $\text{N}_2$  sorption at a relatively high pressure ( $\sim 0.9$  bar) shows the presence of meso- and macrostructures of the PIN- $\text{NH}_2$ . The specific surface area calculated in the relative pressure ( $P/P_0$ ) range from 0.01 to 0.1 shows that the Brunauer-Emmett-Teller (BET) specific surface area of PIN- $\text{NH}_2$  is up to  $480\text{ m}^2\text{ g}^{-1}$ . Additionally, the pore-size distribution (PSD) $^{20}$  calculation result was shown in Fig. 2d and S3 ESI $\dagger$  which indicating the pore diameter is about  $14\text{ \AA}$  and further confirming the microporous feature of the PIN- $\text{NH}_2$ . To gain further insight into the microstructural information, the powder wide-angle X-ray diffraction (PXRD) was further performed on the PIN- $\text{NH}_2$  polymer. As shown in Fig. S4, ESI $\dagger$  only a broad peak at  $17.8^\circ 2\theta$  in the PXRD pattern is present, which clearly suggests that the polymer is mainly amorphous in nature. Additional, the thermogravimetric analysis (TGA) show that the microporous material is stable up to  $370^\circ\text{C}$  indicating its potential in post combustion processes operated at high temperatures (Fig. S5, ESI $\dagger$ ).

Owing to the artful structure design and particular preparation method, there is a reserved aniline group on the side of the indole group in the PIN- $\text{NH}_2$  network. It was expected that after the rapidly capture of the  $\text{CO}_2$  molecule via the  $\pi$ - $\pi$ -stacking interactions, the next aniline group would assist to further stabilize the  $\text{CO}_2$  molecule via hydrogen bonding interactions, in other words, the coefficient effect of  $\pi$ - $\pi$ -stacking interactions and hydrogen bonding interactions would make this porous organic polymer more efficiently attract  $\text{CO}_2$  molecules, which inspires us to investigate the gas uptake capacity. Physisorption isotherms for  $\text{CO}_2$  (at 273 K) measured with a pressure more than 1.0 bar indicated that the resulting PIN- $\text{NH}_2$  network exhibited a high carbon dioxide uptake of 27.7 wt% at 1.0 bar, as shown in Fig. 3a. Comparing with most of reported porous materials such as metal-organic frameworks, $^{21}$  activated carbons, $^{22}$  and microporous organic polymers, $^{23,24}$  the porous organic polymer PIN- $\text{NH}_2$  shows an enhanced  $\text{CO}_2$  uptake (Table S1, ESI $\dagger$ ). The calculation of isosteric heat of adsorption of PIN- $\text{NH}_2$  shows that the heat of adsorption is  $35.7\text{ kJ mol}^{-1}$  (Fig. S6, ESI $\dagger$ ), which is higher than that of the reported azo-linked polymers ( $27.9$ – $29.6\text{ kJ mol}^{-1}$ ), $^{25}$  the acid-functionalized porous polymers ( $32.6\text{ kJ mol}^{-1}$ ), $^{26,27}$  and the indole-based porous polymers. $^{28,29}$  The high value of the heat of adsorption indicated the strong physisorption effect owing to the coefficient effect of  $\pi$ - $\pi$ -stacking interactions and hydrogen bonding interactions.

The application in  $\text{CO}_2$  separation and adsorption field of the traditional POPs is limited in a great degree by the poor gas selectivity as the flue gas and natural gas are both mixed gas. Here, we believed that the  $\text{CO}_2$  can be easily attracted by the heteroaromatic ring via the  $\pi$ - $\pi$ -stacking interactions and then stabilized with the assist of hydrogen bonding interactions, which leading an enhanced gas selectivity. Therefore, we urgently



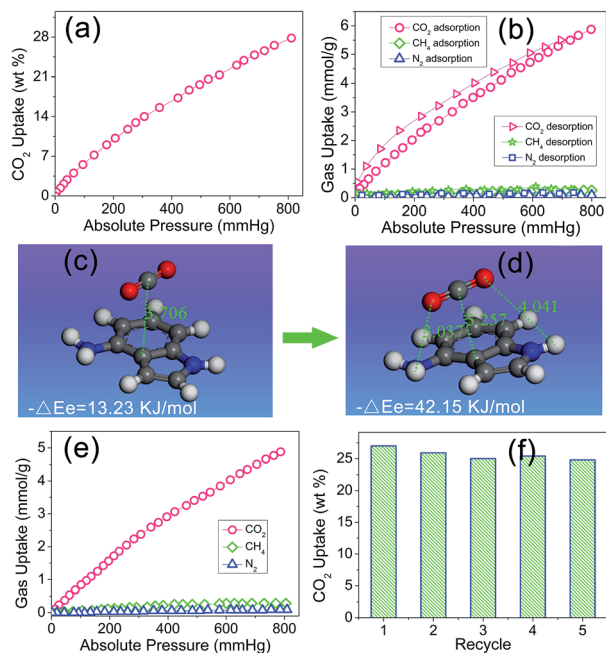


Fig. 3 Gas adsorption isotherms of PIN-NH<sub>2</sub> for CO<sub>2</sub> at 273 K (a), adsorption and desorption isotherms of PIN-NH<sub>2</sub> for different gases at 273 K (b), a CO<sub>2</sub> molecule is adsorbed on the heteroaromatic ring of indole *via*  $\pi$ - $\pi$ -stacking interaction (c) and the CO<sub>2</sub> molecule is further stabilized *via* the coefficient effect of  $\pi$ - $\pi$ -stacking and hydrogen bonding interactions (d), adsorption isotherms of PIN-NH<sub>2</sub> for different gases with 3% RH of water at 273 K (e), reversibility of the PIN-NH<sub>2</sub> polymer in CO<sub>2</sub> capture measured by TGA at 273 K (f).

evaluated the selective gas uptake of the PIN-NH<sub>2</sub> network for small gases (CO<sub>2</sub>/CH<sub>4</sub>, CO<sub>2</sub>/N<sub>2</sub>). In the calculation, the ratio of CO<sub>2</sub>/N<sub>2</sub> is 15/85 and the ratio of CO<sub>2</sub>/CH<sub>4</sub> is 5/95, which is the typical composition of flue gas and natural gas, respectively, the test results were shown in Fig. 3b. It can be found there is a rapid increase for the CO<sub>2</sub> uptake while there is a negligible increase for the CH<sub>4</sub> and N<sub>2</sub> uptake with the increase of the pressure, which maybe due to the unique local dipole- $\pi$  interactions between the porous organic framework PIN-NH<sub>2</sub> and CO<sub>2</sub> molecule. The test results shows that the CO<sub>2</sub> uptake of PIN-NH<sub>2</sub> is up to 5.92 mmol g<sup>-1</sup> at a pressure of 1.0 bar and a temperature of 273 K while the CH<sub>4</sub> and N<sub>2</sub> uptake of PIN-NH<sub>2</sub> is only 0.18 and 0.04 mmol g<sup>-1</sup>, respectively. The estimated ideal CO<sub>2</sub>/CH<sub>4</sub> and CO<sub>2</sub>/N<sub>2</sub> adsorption selectivities are up to 34 and 137, respectively. Additionally, the selectivities of PIN-NH<sub>2</sub> toward CO<sub>2</sub> over CH<sub>4</sub> and N<sub>2</sub> at 291 and 303 K were also investigated, respectively, and the results indicated that the resulting polymer PIN-NH<sub>2</sub> still exhibited good selectivity at higher temperatures (Fig. S7 and S8, ESI†).

The high gas selectivities of this microporous framework may attribute to the strong affinity for CO<sub>2</sub> compared with N<sub>2</sub> and CH<sub>4</sub> arising from the coefficient effect of  $\pi$ - $\pi$ -stacking interactions and hydrogen bonding interactions between the sorbent and CO<sub>2</sub> guest molecule, to further attest the above surmise, we used density functional theory (DFT)<sup>30</sup> at the M06-2X level with the aug-cc-pVDZ basis set to investigate the interaction of aminated indole system with CO<sub>2</sub> and the details

of the calculation is shown in the ESI.† Fig. 3c and d shows the snapshot for CO<sub>2</sub> capture by a model compound. The calculation result shows that owing to the electron-rich and large binding area, the CO<sub>2</sub> was very easily attracted by the indole plane at a distance of 3.706 Å, and the computational binding energy was 13.23 kJ mol<sup>-1</sup> (Fig. 3c). Soon, the balance structure was changed, the CO<sub>2</sub> molecular was moved towards the amino group till the distance between the amino group and CO<sub>2</sub> molecular was 3.037 Å, indicating a hydrogen bonding interaction was formed in this system. As a result, the distance between the indole plane and CO<sub>2</sub> molecular decreased to 3.257 Å from 3.706 Å, and the computational binding energy increased to 42.15 kJ mol<sup>-1</sup>, which meaning a more steady system was formed (Fig. 3d). In the sense of computational chemistry, the expected strong coefficient effect of  $\pi$ - $\pi$ -stacking interactions and hydrogen bonding interactions would favor the uptake of CO<sub>2</sub> of the PIN-NH<sub>2</sub> network. Additional, The DFT result also indicated that the interaction energy between CO<sub>2</sub> and the imine group of indole is relatively weak with a correlation distance at 4.041 Å.

As we all know that the CO<sub>2</sub> adsorption property will be affected in a great degree for porous polymers in the presence of water.<sup>31</sup> In real industrial applications, the flue gas from a power plant is a mixture of CO<sub>2</sub>, water vapor, and others. As a result, it has very important practical significance to study the CO<sub>2</sub> capture performance under humid condition. Here, the CO<sub>2</sub> capture property of PIN-NH<sub>2</sub> was studied at a relative humidity of 3% RH, as shown in Fig. 3e, the CO<sub>2</sub> adsorption capacity of PIN-NH<sub>2</sub> decreased from 5.92 to 4.88 mmol g<sup>-1</sup> (1.0 bar, 273 K), however, the uptake of CH<sub>4</sub> and N<sub>2</sub> does not affected by the water. These results indicate that adsorption of water diminishes the CO<sub>2</sub> capture. Although the selectivity (CO<sub>2</sub>/N<sub>2</sub> = 104, CO<sub>2</sub>/CH<sub>4</sub> = 21) is decreased under humid condition, PIN-NH<sub>2</sub>, to the best of our knowledge, still has very good CO<sub>2</sub> selectivity over other CO<sub>2</sub> capture materials in similar conditions.<sup>32</sup> Moreover, the CO<sub>2</sub> adsorption process is fully reversible (Fig. 3f). Herein, the new aminated indole-based aromatic porous organic polymer PIN-NH<sub>2</sub> synthesized from easily available starting materials demonstrated not only remarkable CO<sub>2</sub> capture capacity, but also prominent CO<sub>2</sub>/N<sub>2</sub> and CO<sub>2</sub>/CH<sub>4</sub> selectivities. Further, the dynamic breakthrough separation experiments of gas mixture at 298 K using a fixed-bed column packed with PIN-NH<sub>2</sub> was carried out to evaluate the performances of PIN-NH<sub>2</sub> aerogel in an actual adsorption-based separation process. The details of the experiment process were described in ESI.† As shown in Fig. S9 and S10, ESI,† the CH<sub>4</sub> and N<sub>2</sub> penetrated through the bed firstly with a retention time for only 6.5 and 3.4 min, respectively, while PIN-NH<sub>2</sub> column can retain CO<sub>2</sub> until above 23 min, which means the high CO<sub>2</sub> adsorption capacity and selectivity of the PIN-NH<sub>2</sub> adsorbent in actual application.

## Conclusions

In this work, we have designed and synthesized a novel aromatic aminated indole-based porous organic polymer PIN-NH<sub>2</sub> *via* Friedel-Crafts alkylation of 4-aminoindole with



formaldehyde dimethyl acetal. FTIR and  $^{13}\text{C}$  CP/MAS NMR characterizations were performed to study the structural information and confirmed the successful formation of the resulting porous organic polymer PIN-NH<sub>2</sub>. The nitrogen adsorption-desorption test shows that the Brunauer–Emmett–Teller (BET) specific surface area of PIN-NH<sub>2</sub> is up to 480 m<sup>2</sup> g<sup>-1</sup> and the thermal analysis indicates that the PIN-NH<sub>2</sub> possesses good thermal stability. More interestingly, we proved that the CO<sub>2</sub> adsorption capacity (27.7 wt%, 1.0 bar, 273 K) and selectivities (CO<sub>2</sub>/N<sub>2</sub> = 137, CO<sub>2</sub>/CH<sub>4</sub> = 34) could be significantly improved may owing to the presence of coefficient effect of  $\pi$ - $\pi$ -stacking interactions and hydrogen bonding interactions between the sorbent and CO<sub>2</sub> guest molecule, making it a promising material for potential application in gas separation. In addition, upon exposure to moisture (RH = 3%), CO<sub>2</sub> capture of the PIN-NH<sub>2</sub> is still highly efficient and selective, with only minor decreases in the CO<sub>2</sub> adsorption capacity and selectivity. Moreover, we demonstrated that the CO<sub>2</sub> adsorption process is fully reversible. The above advantages make the porous organic polymer PIN-NH<sub>2</sub> a outstanding candidate for CO<sub>2</sub> separation material, more importantly, the proposed coefficient effect is expected to be a new rationale for the design and fabrication of CO<sub>2</sub> capture materials for applications in natural gas purification, greenhouse gas reduction, etc.

## Conflicts of interest

There are no conflicts to declare.

## Acknowledgements

This research was financially supported by the National Natural Science Foundation of China (No. U1233202 and No. 51175434). And the Youth Research Foundation of the Civil Aviation Flight University of China (No. Q2019-106), the Laboratory Research Foundation for the State Key Laboratory of Environment-friendly Energy Materials (No. 17kfkf03).

## Notes and references

- 1 T. Gasser, M. Kechiar, P. Ciais, E. J. Burke, T. Kleinen, D. Zhu, Y. Huang, A. Ekici and M. Obersteiner, *Nat. Geosci.*, 2018, **11**, 830.
- 2 A. I. Cooper, *Nature*, 2015, **519**, 294.
- 3 A. Dani, V. Crocellà, C. Magistris, V. Santoro, J. Yuana and S. Bordiga, *J. Mater. Chem. A*, 2017, **5**, 372.
- 4 M. A. Naeem, A. Armutlulu, Q. Imtiaz, F. Donat, R. Schäublin, A. Kierzkowska and C. R. Müller, *Nat. Commun.*, 2018, **9**, 2408.
- 5 L. P. Cavalcanti, G. N. Kalantzopoulos, J. Eckert, K. D. Knudsen and J. O. Fossum, *Sci. Rep.*, 2018, **8**, 11827.
- 6 B. Ghalei, K. Sakurai, Y. Kinoshita, K. Wakimoto, A. P. Isfahani, Q. Song, K. Doitomi, S. Furukawa, H. Hirao, H. Kusuda, S. Kitagawa and E. Sivaniah, *Nat. Energy*, 2017, **2**, 17086.
- 7 G. Rochelle, *Science*, 2009, **325**, 1652.
- 8 G. Chang, Y. Wang, C. Wang, Y. Li, Y. Xu and Li. Yang, *Chem. Commun.*, 2018, **54**, 9785.
- 9 J. Wang, P. Zhang, L. Liu, Y. Zhang, J. Yang, Z. Zeng and S. Deng, *Chem. Eng. J.*, 2018, **348**, 57.
- 10 P. Zhang, Y. Zhong, J. Ding, J. Wang, M. Xu, Q. Deng, Z. Zeng and S. Deng, *Chem. Eng. J.*, 2019, **355**, 963.
- 11 T. Islamoglu, T. Kim, Z. Kahveci, O. M. El-Kadri and H. M. El-Kaderi, *J. Phys. Chem. C*, 2016, **120**, 2592.
- 12 S. Kim and Y. M. Lee, *Prog. Polym. Sci.*, 2015, **43**, 1.
- 13 Z. Xiang, R. Mercado, J. M. Huck, H. Wang, Z. Guo, W. Wang, D. Cao, M. Haranczyk and B. Smit, *J. Am. Chem. Soc.*, 2015, **137**, 13301.
- 14 G. Chang, L. Yang, J. Yang, M. P. Stoykovich, X. Deng, J. Cui and D. Wang, *Adv. Mater.*, 2018, **30**, 1704234.
- 15 P. Yang, L. Yang, Y. Wang, L. Song, J. Yang and G. Chang, *J. Mater. Chem. A*, 2019, **7**, 531.
- 16 R. W. Flaig, T. M. Osborn Popp, A. M. Fracaroli, E. A. Kapustin, M. J. Kalmutzki, R. M. Altamimi, F. Fathieh, J. A. Reimer and O. M. Yaghi, *J. Am. Chem. Soc.*, 2017, **139**, 12125.
- 17 H. Thakkar, S. Eastman, A. Al-Mamoori, A. Hajari, A. A. Rownaghi and F. Rezaei, *ACS Appl. Mater. Interfaces*, 2017, **9**, 7489.
- 18 A. Alabadi, H. A. Abbood, Q. Li, N. Jing and B. Tan, *Nature*, 2016, **6**, 38614.
- 19 L. Yang, G. Chang and D. Wang, *ACS Appl. Mater. Interfaces*, 2017, **9**, 15213.
- 20 A. Vishnyakov, P. I. Ravikovitch and A. V. Neimark, *Langmuir*, 1999, **15**, 8736.
- 21 J. Liu, P. K. Thallapally, B. P. McGrail and D. R. Brown, *Chem. Soc. Rev.*, 2012, **41**, 2308.
- 22 B. S. Ghanem, M. Hashem, D. M. Harris, K. J. Msayib, M. Xu, P. M. Budd, N. Chaukura, D. Book, S. Tedds, A. Walton and N. B. McKeown, *Macromolecules*, 2010, **43**, 5287.
- 23 X. S. Ding, H. Li, Y. C. Zhao and B. H. Han, *Polym. Chem.*, 2015, **6**, 5305.
- 24 C. Zhang, P. C. Zhu, L. X. Tan, L. N. Luo, Y. Liu, J. M. Liu, S. Y. Ding, B. X. Tan, L. Yang and H. B. Xu, *Polymer*, 2016, **82**, 100.
- 25 J. Lu and J. Zhang, *J. Mater. Chem. A*, 2014, **2**, 13831.
- 26 R. Dawson, D. J. Adams and A. I. Cooper, *Chem. Sci.*, 2011, **2**, 1173.
- 27 W. Lu, D. Yuan, J. Sculley, D. Zhao, R. Krishna and H. C. Zhou, *J. Am. Chem. Soc.*, 2011, **133**, 18126.
- 28 G. Chang, Z. Shang, Y. Tao and L. Yang, *J. Mater. Chem. A*, 2016, **4**, 2517.
- 29 G. Chang, L. Yang, J. Yang, Y. Huang, K. Cao, J. Ma and D. Wang, *Polym. Chem.*, 2016, **7**, 5768.
- 30 C. Balzer, R. T. Cimino, G. Y. Gor, A. V. Neimark and G. Reichenauer, *Langmuir*, 2016, **32**, 8265.
- 31 A. C. Kizzie, A. G. Wong-Foy and A. J. Matzger, *Langmuir*, 2011, **27**, 6368.
- 32 J. Liu, J. Tian, P. K. Thallapally and B. P. McGrail, *J. Phys. Chem. C*, 2012, **116**, 9575.

